2011 IEEE 12th International Workshop on Signal Processing Advances in Wireless Communications

Rate-Adaptive Modulation for Square OSTBCs in Arbitrarily Correlated Rayleigh Fading With Imperfect Channel Estimation

Lennert Jacobs and Marc Moeneclaey
Ghent University, TELIN Department, DIGCOM Group
St-Pietersnieuwstraat 41, B-9000 Gent, Belgium
Email: {Lennert.Jacobs,mm}@telin.ugent.be

Andrea Conti
University of Ferrara, ENDIF
Via Saragat 1, 44100 Ferrara, Italy
Email: a.conti@ieee.org

Abstract—**Multiple-input multiple-output (MIMO) systems employing adaptive modulation have been widely used for their potential to optimize the spectral efficiency while keeping the bit error probability (BEP) under a certain target level. In this paper, we examine a MIMO system using square orthogonal space-time block codes (OSTBCs) with rate-adaptive M-QAM and operating over arbitrarily correlated Rayleigh fading channels with imperfect channel estimation. Assuming finite-rate feedback without delay, we derive accurate closed-form expressions for the average BEP, spectral efficiency and bit error outage of our system. The presented expressions allow to easily study the impact of channel estimation errors and fading correlation on the performance of rate-adaptive MIMO OSTBC systems.**

I. Introduction

It is well understood that multiple-input multiple-output (MIMO) systems employing space-time coding enhance the performance of wireless communication systems by taking advantage of the spatial diversity [1]. By providing the transmitter with information about the channel state, the effect of time-varying fading can be mitigated by adapting transmission parameters such as the constellation size, the coding rate or the transmit power [2].

Due to its high spectral efficiency (SE), M-ary quadrature amplitude modulation (M-QAM) has been adopted in various standards, e.g., DVB, WLAN and LTE. In [3], closed-form expressions for the average bit error probability (BEP) and SE are derived for a rate-adaptive M-QAM system employing orthogonal space-time block coding with outdated, finite-rate feedback over independent and identically distributed (i.i.d.) flat Rayleigh fading channels. Closed-form expressions for the average SE of two rate-adaptive MIMO schemes, i.e., orthogonal space-time block codes (OSTBCs) and spatial multiplexing with zero-forcing receiver were derived in [4] for i.i.d. Rayleigh fading channels with imperfect channel state information (CSI). It also considers a novel adaptation scheme that enables the receiver to switch between OSTBCs and spatial multiplexing. In [5], a similar analysis was given for the case of spatially correlated Rayleigh fading channels with transmit correlation and perfect CSI. Closed-form expressions of the average BEP, SE and outage probability of rate-adaptive OSTBC systems were given in [6] for spatially correlated Rayleigh channels with and without perfect CSI. However, in [6] the instantaneous BEP is approximated by an exponential function, which simplifies the analysis significantly but can be not sufficiently accurate for the performance evaluation in fading channels. Bounds and approximations for the BEP of QAM systems with diversity are analyzed in [7].

In this paper, we present a novel and accurate closed-form expression for the average BEP of a rate-adaptive MIMO OSTBC system with imperfect CSI in arbitrarily correlated Rayleigh fading channels. For the case of i.i.d. Rayleigh fading channels, an exact closed-form expression is provided. In addition, we provide a simple approximate closed-form expression for the average BEP, which yields more accurate results than the approximate expression from [6]. To guarantee a fair comparison between different channel estimation scenarios, the performance is compared given a fixed total energy for both data and pilot symbols, and the achieved spectral efficiency (ASE) is considered rather than the SE. Our analysis enables system designers to choose appropriate system parameters considering the trade-off between SE and outage for a given target BEP.

II. System model

A. Transmitter

We consider a MIMO OSTBC system with L_{t} transmit and L_{r} receive antennas. A square OSTBC from a complex orthogonal design [1] is defined by an $L_{\mathrm{t}} \times L_{\mathrm{t}}$ coded symbol matrix $\mathbf{C}$, the entries of which are linear combinations of N_{s} information symbols s_i, $1 \leq i \leq N_{\mathrm{s}}$, and their complex conjugate s_i^*, such that

$$\mathbf{C} = \sum_{i=1}^{N_{\mathrm{s}}} \left(\mathbf{C}_i \, s_i + \mathbf{C}_i^{'} \, s_i^* \right) \tag{1}$$

where $\mathbf{C}_i$ and $\mathbf{C}_i^{'}$ are $L_{\mathrm{t}} \times L_{\mathrm{t}}$ matrices that comprise the coefficients of s_i and s_i^*, respectively. $\mathbf{C}$ is assumed to be scaled in such way that it satisfies

$$\mathbf{C}^H \mathbf{C} = \mathbf{C}\,\mathbf{C}^H = \lambda \,\|\mathbf{s}\|^2 \,\mathbf{I}_{L_{\mathrm{t}}} \tag{2}$$

where the superscript H denotes the conjugate transpose operator, $\lambda \triangleq L_\mathrm{t}/N_\mathrm{s}$, $\mathbf{s} = [s_1, s_2, \ldots, s_{N_\mathrm{s}}]^T$ is the data symbol vector, and $\mathbf{I}_{L_\mathrm{t}}$ denotes the $L_\mathrm{t} \times L_\mathrm{t}$ identity matrix. The transmitter uses data frames consisting of K/L_t code matrices $\mathbf{C}$, with K being a multiple of L_t. In this way, K coded data symbols per transmit antenna are sent within one frame. To estimate the channel, K_p pilot symbols per transmit antenna are transmitted prior to the data frame. We consider orthogonal pilot sequences, i.e., the $L_\mathrm{t} \times K_\mathrm{p}$ pilot matrix $\mathbf{C}_\mathrm{p}$ satisfies

$$\mathbf{C}_\mathrm{p}\mathbf{C}_\mathrm{p}^H = K_\mathrm{p}\mathbf{I}_{L_\mathrm{t}}. \tag{3}$$

B. Channel model

The MIMO channel is represented by the $L_\mathrm{r} \times L_\mathrm{t}$ complex-valued random matrix $\mathbf{H}$, which is assumed to remain constant during the transmission of K_p pilot symbols and K information symbols. When stacking the elements of $\mathbf{H}$ into the vector $\mathbf{h} \triangleq \mathrm{vec}(\mathbf{H})$ of dimension $L = L_\mathrm{t}L_\mathrm{r}$, the elements of $\mathbf{h}$ are arbitrarily correlated zero-mean (ZM) circularly symmetric complex Gaussian (CSCG) random variables (RVs) with a positive definite covariance matrix $\boldsymbol{\mathcal{R}}_{\mathbf{hh}} \triangleq \mathbb{E}[\mathbf{h}\,\mathbf{h}^H]$. The receiver observes the $(L_\mathrm{r}K_\mathrm{p})$-dimensional column vector

$$\mathbf{r}_\mathrm{p} = \sqrt{E_\mathrm{p}}\,\mathbf{B}_\mathrm{p}\,\mathbf{h} + \mathbf{w}_\mathrm{p} \tag{4a}$$

from which the channel is estimated, and an L-dimensional column vector $\mathbf{r}$ for each transmitted code matrix $\mathbf{C}$, given by

$$\mathbf{r} = \sqrt{E_\mathrm{s}}\,\mathbf{B}\,\mathbf{h} + \mathbf{w} \tag{4b}$$

where the vectors $\mathbf{w}_\mathrm{p}$ and $\mathbf{w}$ consist of i.i.d. ZM CSCG RVs with variance N_0; $\mathbf{B}_\mathrm{p}$ and $\mathbf{B}$ are defined as $\mathbf{B}_\mathrm{p} \triangleq \mathbf{C}_\mathrm{p}^T \otimes \mathbf{I}_{L_\mathrm{r}}$ and $\mathbf{B} \triangleq \mathbf{C}^T \otimes \mathbf{I}_{L_\mathrm{r}}$, respectively, with $\otimes$ denoting the Kronecker matrix product. Assuming that $\mathbb{E}\left[\|s_i\|^2\right] = 1$, E_p and E_s in (4a) and (4b) denote the average pilot and data symbol energy, respectively.

Note that $L_\mathrm{t}K_\mathrm{p}$ pilot symbols and $L_\mathrm{t}K$ coded data symbols are required to transmit $N_\mathrm{s}K/L_\mathrm{t}$ information symbols. Let E_d be the average total energy needed to transmit one information symbol, such that the average total energy devoted to the transmission of one data frame is given by $E_\mathrm{tot} \triangleq (N_\mathrm{s}K/L_\mathrm{t})E_\mathrm{d}$. By allocating a large fraction of E_tot to pilot symbols, very accurate channel estimation can be obtained. However, the more energy is devoted to pilot symbols, the less energy remains available for data transmission, calling for a trade-off between resources dedicated to pilot and data symbols for a set of target performance metrics [8], [9]. The relation between E_s and E_d is given by

$$E_\mathrm{s} = \frac{K}{K + \epsilon K_\mathrm{p}}\rho E_\mathrm{d}, \tag{5}$$

where $\epsilon \triangleq E_\mathrm{p}/E_\mathrm{s}$ and $\rho \triangleq N_\mathrm{s}/L_\mathrm{t}^2$ denote the ratio of E_p to E_s and the code rate, respectively.

C. Mismatched receiver

Using the vector channel model (4a), the linear minimum mean-square error (LMMSE) channel estimate is given by [9]

$$\hat{\mathbf{h}} = \frac{1}{K_\mathrm{p}\sqrt{E_\mathrm{p}}}\left(\frac{N_0}{K_\mathrm{p}E_\mathrm{p}}\mathbf{I}_L + \boldsymbol{\mathcal{R}}_{\mathbf{hh}}\right)^{-1}\boldsymbol{\mathcal{R}}_{\mathbf{hh}}\,\mathbf{B}_\mathrm{p}^H\,\mathbf{r}_\mathrm{p}. \tag{6}$$

The components of $\hat{\mathbf{h}}$ are shown to be ZM CSCG RVs with covariance matrix given by [10]

$$\boldsymbol{\mathcal{R}}_{\hat{\mathbf{h}}\hat{\mathbf{h}}} \triangleq \mathbb{E}\left[\hat{\mathbf{h}}\,\hat{\mathbf{h}}^H\right] = \boldsymbol{\mathcal{R}}_{\mathbf{hh}}\boldsymbol{\mathcal{R}}_{\mathbf{hh}}\left(\frac{N_0}{K_\mathrm{p}E_\mathrm{p}}\mathbf{I}_L + \boldsymbol{\mathcal{R}}_{\mathbf{hh}}\right)^{-1}. \tag{7}$$

We consider a mismatched maximum-likelihood (ML) receiver that uses the estimated channel (6) instead of the true channel. Taking (2) into account, it is readily verified that the detection algorithm for the information symbols s_i reduces to symbol-by-symbol detection

$$\hat{s}_i = \arg\min_{\tilde{s}} |u_i - \tilde{s}|, \qquad 1 \le i \le N_\mathrm{s} \tag{8}$$

where the minimization is over the symbols $\tilde{s}$ belonging to the considered constellation and the decision variables u_i are given by

$$u_i = \frac{\hat{\mathbf{h}}^H\left(\mathbf{C}_i^* \otimes \mathbf{I}_{L_\mathrm{r}}\right)\mathbf{r} + \mathbf{r}^H\left(\mathbf{C}_i^{'T} \otimes \mathbf{I}_{L_\mathrm{r}}\right)\hat{\mathbf{h}}}{\lambda\sqrt{E_\mathrm{s}}\|\hat{\mathbf{h}}\|^2}. \tag{9}$$

III. Adaptive Modulation Schemes

We consider a rate-adaptive MIMO OSTBC system, where the receiver selects a constellation size M_j to be used by the transmitter from a finite set of candidates $\mathcal{M} = \{M_0, M_1, \ldots, M_J\}$ with Gray mapping, and sends this information back to the transmitter over a perfect feedback channel without delay. When fast adaptive modulation (FAM) is applied, the constellation size M_j is chosen depending on the value of the estimated instantaneous SNR $\hat{\gamma} = \|\hat{\mathbf{h}}\|^2\frac{E_\mathrm{s}}{N_0}$. Another approach consists in adapting M_j based on tracking of large-scale fading. Analysis of fast and slow adaptive modulation with diversity is given in [11]. Here, the modulation level M_j is selected when $\hat{\gamma}$ falls in the interval $[\hat{\gamma}_j^\star, \hat{\gamma}_{j+1}^\star)$, where $\hat{\gamma}_{J+1}^\star = \infty$ and the switching thresholds $\hat{\gamma}_j^\star$, $j = 0, \ldots, J$, are chosen to provide a given instantaneous target BEP $P_\mathrm{b}^\star$

$$P_\mathrm{b}(\hat{\gamma}_j^\star, M_j) = P_\mathrm{b}^\star \tag{10}$$

where $P_\mathrm{b}(\hat{\gamma}, M_j)$ denotes the BEP for M_j-QAM with imperfect channel estimation as a function of the estimated instantaneous SNR $\hat{\gamma}$. When even the smallest constellation size M_0 does not meet the target BEP, i.e., when $\hat{\gamma} < \hat{\gamma}_0^\star$, no data are transmitted and the system is in outage.

IV. Performance Evaluation

In this section, we derive closed-form expressions for the resulting average BEP, ASE, and BEO of a rate-adaptive MIMO OSTBC system with LMMSE channel estimation.

In [10], it is shown that for square M-QAM constellations with equally likely symbol vectors $\mathbf{s}$, the instantaneous BEP $P_{\mathrm{b},j}(\hat{\gamma})$ can be calculated as

$$P_\mathrm{b}(\hat{\gamma}, M) = \frac{2}{M^{N_\mathrm{s}}}\sum_{\mathbf{s}\in\Psi^{N_\mathrm{s}}}\sum_{b_\mathrm{R}\in\Psi_\mathrm{R}}\frac{d_\mathrm{H}(s_{i,\mathrm{R}}, b_\mathrm{R})}{\log_2 M}P_{i,\mathrm{R}}(\mathbf{s}, b_\mathrm{R}, \hat{\gamma}) \tag{11}$$

where Ψ and Ψ_R represent the sets of the M-QAM constellation points and their real parts, respectively, and $d_\mathrm{H}(s_{i,\mathrm{R}}, b_\mathrm{R})$

$$I(a,b,c,\beta,L) \triangleq Q\left(\sqrt{\beta a}\right)\exp\left(-\frac{a}{c}\right)\sum_{k=0}^{L-1}\frac{1}{k!}\left(\frac{a}{c}\right)^k - Q\left(\sqrt{\beta b}\right)\exp\left(-\frac{b}{c}\right)\sum_{k=0}^{L-1}\frac{1}{k!}\left(\frac{b}{c}\right)^k$$
$$- \sqrt{\frac{\beta c}{2+\beta c}}\left(Q(t_1)-Q(t_2)\right)\sum_{k=0}^{L-1}\frac{1}{2^k}\binom{2k}{k}\frac{1}{(2+\beta c)^k}$$
$$- \frac{1}{\sqrt{2\pi}}\sqrt{\frac{\beta c}{2+\beta c}}\left[\sum_{k=1}^{L-1}\frac{1}{2^k}\binom{2k}{k}\frac{1}{(2+\beta c)^k}\sum_{i=1}^{k}2^{i-1}\frac{(i-1)!}{(2i-1)!}\left(\exp\left(-\frac{t_1^2}{2}\right)t_1^{2i-1} - \exp\left(-\frac{t_2^2}{2}\right)t_2^{2i-1}\right)\right]. \quad (12)$$

denotes the Hamming distance between the in-phase bits allocated to s_i and a QAM symbol $b = b_\mathrm{R} + jb_\mathrm{I}$. $P_{i,\mathrm{R}}(\mathbf{s}, b_\mathrm{R}, \hat{\gamma})$ is the probability that the real part of the decision variable (9) is located inside the projection on the real axis of the decision area of b, when $\mathbf{s}$ and $\hat{\gamma}$ are known. With $d_1(s_{i,\mathrm{R}}, b_\mathrm{R})$ and $d_2(s_{i,\mathrm{R}}, b_\mathrm{R})$ denoting the distances between $s_{i,\mathrm{R}}$ and the boundaries of the projection of the decision area of b, with $d_1(s_{i,\mathrm{R}}, b_\mathrm{R}) < d_2(s_{i,\mathrm{R}}, b_\mathrm{R})$, $P_{i,\mathrm{R}}(\mathbf{s}, b_\mathrm{R}, \hat{\gamma})$ is given by

$$P_{i,\mathrm{R}}(\mathbf{s}, b, \hat{\gamma}) = Q\left(\frac{d_1(s_{i,\mathrm{R}}, b_\mathrm{R})}{\sigma_{i,\mathrm{R}}(\mathbf{s},\hat{\gamma})}\right) - Q\left(\frac{d_2(s_{i,\mathrm{R}}, b_\mathrm{R})}{\sigma_{i,\mathrm{R}}(\mathbf{s},\hat{\gamma})}\right) \quad (13)$$

where $Q(.)$ is the Gaussian Q-function. For i.i.d. Rayleigh fading, $\sigma^2_{i,\mathrm{R}}(\mathbf{s},\hat{\gamma})$ is given by [12]

$$\sigma^2_{i,\mathrm{R}}(\mathbf{s},\hat{\gamma}) = \frac{1}{2\lambda\hat{\gamma}}\left(1 + \frac{\lambda\|\mathbf{s}\|^2}{\frac{N_0}{E_\mathrm{s}} + \epsilon K_\mathrm{p}}\right) \quad (14)$$

whereas it is shown in [10] that for arbitrarily correlated Rayleigh fading and $\epsilon K_\mathrm{p}\frac{E_\mathrm{s}}{N_0} \gg 1$, $\sigma^2_{i,\mathrm{R}}(\mathbf{s},\hat{\gamma})$ results in

$$\sigma^2_{i,\mathrm{R}}(\mathbf{s},\hat{\gamma}) \approx \frac{1}{2\lambda\hat{\gamma}}\left(1 + \frac{\lambda\|\mathbf{s}\|^2}{\epsilon K_\mathrm{p}}\right). \quad (15)$$

For a given target BEP, the switching thresholds can be computed off-line by substituting (11) into (10) and numerically solving the resulting equation.

Since the constellation size is selected based on the estimated instantaneous SNR $\hat{\gamma}$, the average BEP is given by

$$\overline{\mathrm{BEP}} = \frac{\sum_{j=0}^{J} R_j \int_{\hat{\gamma}_j^\star}^{\hat{\gamma}_{j+1}^\star} P_\mathrm{b}(x, M_j)\, p_{\hat{\gamma}}(x)\,\mathrm{d}x}{\sum_{j=0}^{J} R_j \int_{\hat{\gamma}_j^\star}^{\hat{\gamma}_{j+1}^\star} p_{\hat{\gamma}}(x)\,\mathrm{d}x}. \quad (16)$$

where $R_j \triangleq \log_2(M_j)$ and $p_{\hat{\gamma}}(x)$ is the probability density function (PDF) of $\hat{\gamma}$. The ASE is defined as η times the SE, where $\eta \triangleq K/(K + K_\mathrm{p})$ represents the fraction of the resources that is used for the transmission of the data-dependent portion of the frame [13]. Hence, the average ASE (in bits/s/Hz) is obtained as

$$\overline{\mathrm{ASE}} = \frac{K}{K+K_\mathrm{p}}\frac{N_\mathrm{s}}{L_\mathrm{t}}\sum_{j=0}^{J} R_j \int_{\hat{\gamma}_j^\star}^{\hat{\gamma}_{j+1}^\star} p_{\hat{\gamma}}(x)\,\mathrm{d}x. \quad (17)$$

Since the BEO is given by the probability that the BEP exceeds a target value $P_\mathrm{b}^\star$ [6], [14], [15], it results in

$$\mathrm{BEO} = \int_0^{\hat{\gamma}_0^\star} p_{\hat{\gamma}}(x)\,\mathrm{d}x. \quad (18)$$

Using a moment generating function (MGF) approach, the PDF $p_{\hat{\gamma}}(x)$ of the estimated instantaneous SNR is easily obtained as [16]

$$p_{\hat{\gamma}}(x) = \sum_{m=1}^{\kappa}\sum_{n=1}^{c_m} D_{m,n}\frac{x^{n-1}\exp\left(-\frac{x}{\lambda_m\frac{E_\mathrm{s}}{N_0}}\right)}{(n-1)!\left(\lambda_m\frac{E_\mathrm{s}}{N_0}\right)^n} \quad (19)$$

where $x \geq 0$ and λ_m's, $m = 1, 2, \ldots, \kappa$, are the distinct eigenvalues of $\boldsymbol{\mathcal{R}}_{\hat{\mathbf{h}}\hat{\mathbf{h}}}$ given by (7), with corresponding algebraic multiplicities c_m. In (19), the parameters $D_{m,n}$ are given by

$$D_{m,n} = \frac{(\lambda_m)^{n-c_m}}{(c_m-n)!}\left[\frac{\mathrm{d}^{c_m-n}}{\mathrm{d}s^{c_m-n}}\Psi_m(s)\right]\Big|_{s=-\frac{1}{\lambda_m}} \quad (20)$$

where

$$\Psi_m(s) = \prod_{\substack{l=1\\ l\neq m}}^{\kappa}\left(1+\lambda_l\, s\right)^{-c_l}. \quad (21)$$

In order to obtain the numerator of (16), we present the following closed-form solution, which to the best of our knowledge has not appeared in the literature before

$$\frac{1}{c^n(L-1)!}\int_a^b Q\left(\sqrt{\beta y}\right)y^{L-1}\exp\left(-\frac{y}{c}\right)\mathrm{d}y = I(a,b,c,\beta,L), \quad (22)$$

where $I(a,b,c,\beta,L)$ is defined in (12), with $t_1 \triangleq \sqrt{\beta a + 2a/c}$ and $t_2 \triangleq \sqrt{\beta b + 2b/c}$. In this way, a closed-form expression for the integral in the numerator of (16) can be obtained from (11)-(15) and (19). Closed-form expressions for the integrals in the denominator of (16) and in (17)-(18) can be obtained using (19) and the lower incomplete gamma function $\gamma(s,x)$, which is defined as

$$\gamma(s,x) \triangleq \int_0^x t^{s-1}\exp\left(-t\right)\mathrm{d}t. \quad (23)$$

The complexity of the resulting closed-form expression for the average BEP can be further reduced by replacing $\|\mathbf{s}\|^2$ in (14) or (15) by its expectation $\mathbb{E}[\|\mathbf{s}\|^2] = N_\mathrm{s}$. In this way, the summation over the data symbol vector $\mathbf{s}$ in (11) reduces to a summation over $s_{i,\mathrm{R}}$, which reduces the computational complexity of both the instantaneous and average BEP considerably. The impact of this approximation on the accuracy of the resulting average BEP expression is illustrated in Section V.

V. Numerical results

We report numerical results for a rate-adaptive MIMO OSTBC system using Alamouti's code [1] ($L_{\rm t} = N_{\rm s} = 2$). We assume that $E_{\rm p} = E_{\rm s}$, and that the constellation set is given by $\mathcal{M} = \{4, 16, 64\}$. To maximize the ASE for a given target BEP, the number of pilot symbols $K_{\rm p}$ is optimized with respect to the number of coded data symbols K. With larger $K_{\rm p}$, more accurate CSI can be obtained, which reduces the BEO and enables larger constellations to meet the target BEP. However, as mentioned in Section II-B, increasing $K_{\rm p}$ also reduces $E_{\rm s}$ and the ASE, according to (17), because more resources are wasted on pilot symbols. Hence, $K_{\rm p}$ needs to be carefully selected. We choose $K = 20$ and $K_{\rm p} = 4$, which can be shown to be a good trade-off between BEO and SE.

In Section IV, we have shown how the average BEP can be derived from the instantaneous BEP and the PDF of the estimated instantaneous SNR $\hat{\gamma}$. In Fig. 1, several analytical average BEP curves are presented, corresponding to different approximations of the instantaneous BEP $P_{\rm b}(\hat{\gamma}, M)$: (a) the closed-form expression (11) using the approximation in (15); (b) the approximation of (11) discussed in the last paragraph of Section IV; and (c) the exponential approximation of $P_{\rm b}(\hat{\gamma}, M)$, as used in [6]. The dots in the figure represent brute-force simulation results, which show a good agreement with the analytical curves. A mismatched single-antenna receiver ($L_{\rm r} = 1$) with a covariance matrix given by

$$\boldsymbol{\mathcal{R}}_{\mathbf{hh}} = \begin{pmatrix} 1 & 0.6 \\ 0.6 & 1 \end{pmatrix} \tag{24}$$

is considered. The results are shown for both a target BEP of $P_{\rm b}^{\star} = 10^{-3}$ and $P_{\rm b}^{\star} = 10^{-4}$. From the brute-force simulation results, it follows that the presented average BEP (a) resulting from (11) and (15) is very accurate for moderate to high average SNR, whereas the approximations of the instantaneous BEP used to obtain (b) and (c) cause a shift of the resulting average BEP curves. For a target BEP of $P_{\rm b}^{\star} = 10^{-4}$, the average BEP curve from (b) turns out to be more accurate than the BEP (c) from [6], while both expressions have a similar computational complexity. For low average SNR, the average BEP curves from (a), (b), and (c) diverge from the simulations because of the high-SNR approximations used to obtain (15) or (11). In case of a rate-adaptive system, however, the low SNR region is not of particular interest, as the BEO would be very high and, consequently, the resulting average ASE very low.

For the remaining numerical results, we will apply a target BEP of $P_{\rm b}^{\star} = 10^{-4}$. Fig. 2 shows the average BEP, ASE, and BEO curves for several values of $L_{\rm r}$ under the assumption of i.i.d. Rayleigh fading with $\boldsymbol{\mathcal{R}}_{\mathbf{hh}} = \mathbf{I}_{2L_{\rm r}}$. Using (11) and (14), the exact average BEP can be obtained. The performance results are shown for both a receiver with perfect CSI and a mismatched receiver with LMMSE channel estimation. It is observed from the figure that both imperfect CSI and the number of receive antennas $L_{\rm r}$ have a considerable impact on the ASE and the BEO. Imperfect CSI reduces the ASE significantly since channel estimation errors and the energy devoted to pilot symbols give rise to a degradation of the instantaneous BEP, such that, compared to the case of perfect CSI, often a smaller constellation has to be selected in order to satisfy the target BEP constraint. Moreover, the transmission of pilot symbols reduces the ASE by a factor $K/(K + K_{\rm p})$ because part of the resources that could be used for data symbols are now occupied by pilot symbols. On the other hand, increasing the number of receive antennas increases the ASE since the provided spatial diversity mitigates fading, such that often a larger constellation can be selected which still satisfies the target BEP constraint.

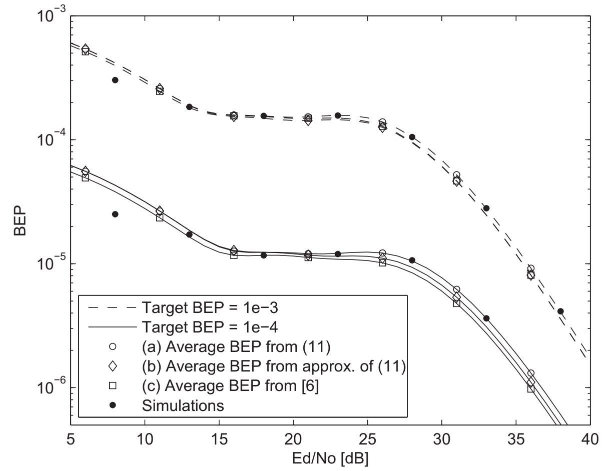

Fig. 1. Average BEP of Alamouti's code under correlated Rayleigh fading, for both a target BEP of $P_{\rm b}^{\star} = 10^{-3}$ and $P_{\rm b}^{\star} = 10^{-4}$.

Fig. 3 shows the average BEP, ASE and BEO for a dual-antenna receiver ($L_{\rm r} = 2$) under correlated Rayleigh fading with $\boldsymbol{\mathcal{R}}_{\mathbf{hh}} = \boldsymbol{\mathcal{R}}_{\rm t} \otimes \boldsymbol{\mathcal{R}}_{\rm r}$, where $\boldsymbol{\mathcal{R}}_{\rm t}$ and $\boldsymbol{\mathcal{R}}_{\rm r}$ are given by

$$\boldsymbol{\mathcal{R}}_{\rm t} = \boldsymbol{\mathcal{R}}_{\rm r} = \begin{pmatrix} 1 & \rho \\ \rho & 1 \end{pmatrix} \tag{25}$$

and ρ denotes the correlation factor. The results are shown for both a receiver with perfect CSI and a mismatched receiver with LMMSE channel estimation, and for $\rho \in \{0, 0.3, 0.8\}$. Note that $\rho = 0$ corresponds to the case of i.i.d. fading. We observe that for low correlation levels, i.e., $\rho < 0.3$, the impact of correlation on the ASE and BEO is fairly negligible. For high correlation, however, e.g., $\rho = 0.8$, the ASE and BEO are clearly negatively affected by fading correlation.

VI. Conclusion

In this paper, we investigated the effect of imperfect channel estimation and fading correlation on the performance of a rate-adaptive MIMO OSTBC system. Assuming finite-rate feedback without delay, we presented accurate closed-form expressions for the average BEP, ASE, and BEO, which enable the design of such adaptive communication systems.

Acknowledgments

This work was supported by the European Commission in the framework of the FP7 Network of Excellence in Wireless

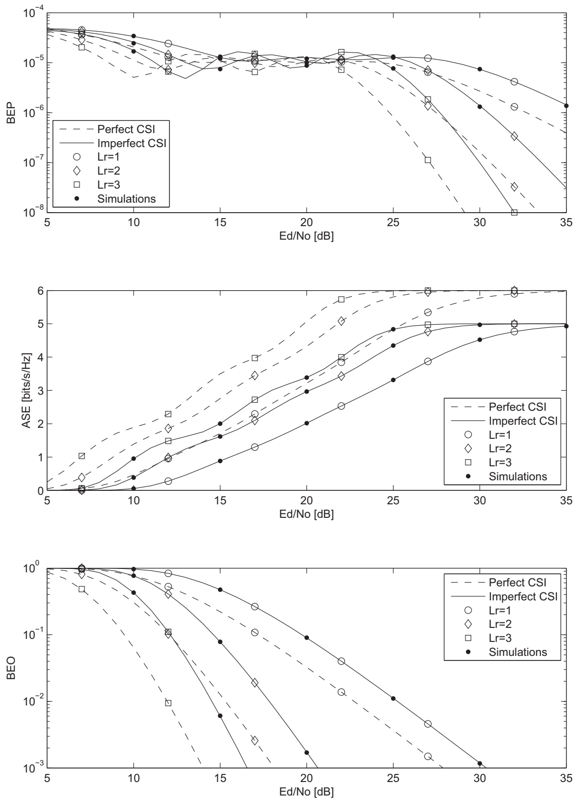

Fig. 2. Average BEP, ASE and BEO of Alamouti's code under i.i.d. Rayleigh fading, for perfect and imperfect CSI, and for $L_r \in \{1, 2, 3\}$.

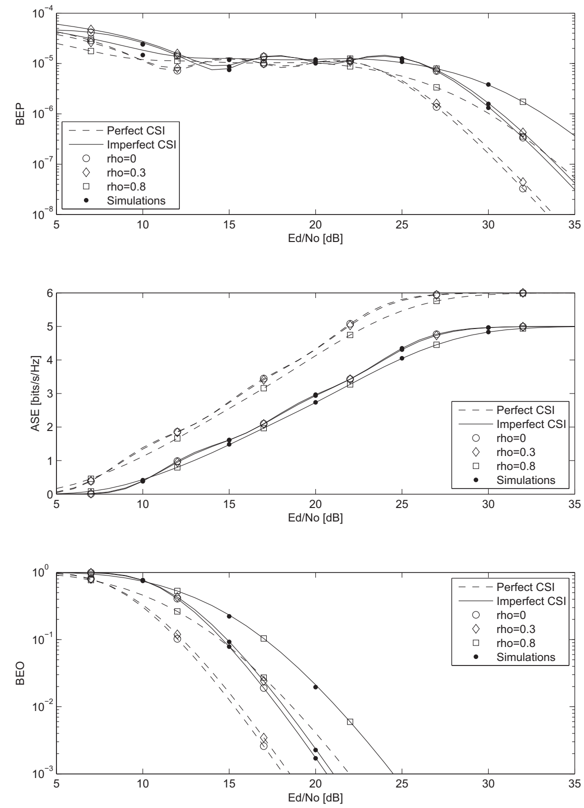

Fig. 3. Average BEP, ASE and BEO of Alamouti's code under correlated Rayleigh fading with $\rho \in \{0, 0.3, 0.8\}$, and for perfect and imperfect CSI.

COMmunications NEWCOM++ (contract no. 216715). The first author also gratefully acknowledges the support from the Fund for Scientific Research in Flanders (FWO-Vlaanderen).

REFERENCES

[1] V. Tarokh, H. Jafarkhani, and A. R. Calderbank, "Space-time block codes from orthogonal designs," *IEEE Trans. Inform. Theory*, vol. 45, no. 5, pp. 1456–1467, Jul. 1999.

[2] A. Goldsmith and S.-G. Chua, "Variable-rate variable-power MQAM for fading channels," *IEEE Trans. Commun.*, vol. 45, no. 10, pp. 1218 –1230, Oct. 1997.

[3] Y. Ko and C. Tepedelenlioglu, "Orthogonal space-time block coded rate-adaptive modulation with outdated feedback," *IEEE Trans. Wireless Commun.*, vol. 5, no. 2, pp. 290 – 295, Feb. 2006.

[4] J. Huang and S. Signell, "Impact of channel estimation error on performance of adaptive MIMO systems," in *proc. IEEE Int. Conf. on Acoustics, Speech and Signal Processing (ICASSP)*, Mar. 2008, pp. 2865 –2868.

[5] ——, "On spectral efficiency of low-complexity adaptive MIMO systems in Rayleigh fading channel," *IEEE Trans. Wireless Commun.*, vol. 8, no. 9, pp. 4369–4374, Sep. 2009.

[6] ——, "On performance of adaptive modulation in MIMO systems using orthogonal space-time block codes," *IEEE Trans. Veh. Technol.*, vol. 58, no. 8, pp. 4238 –4247, Oct. 2009.

[7] A. Conti, M. Win, and M. Chiani, "Invertible bounds for M-QAM in rayleigh fading," *IEEE Trans. Wireless Commun.*, vol. 4, no. 5, pp. 1994–2000, Sep. 2005.

[8] M. Chiani, A. Conti, and C. Fontana, "Improved performance in td-cdma mobile radio system by optimizing energy partition in channel estimation," *IEEE Trans. Commun.*, vol. 51, no. 3, pp. 352 – 355, Mar. 2003.

[9] G. Taricco, "Optimum receiver design and performance analysis of arbitrarily correlated rician fading MIMO channels with imperfect channel state information," *IEEE Trans. Inform. Theory*, vol. 56, no. 3, pp. 1114–1134, Mar. 2010.

[10] L. Jacobs and M. Moeneclaey, "BER analysis of square OSTBCs with LMMSE channel estimation in arbitrarily correlated Rayleigh fading channels," *IEEE Commun. Lett.*, vol. 14, no. 7, pp. 626 –628, Jul. 2010.

[11] A. Conti, M. Z. Win, and M. Chiani, "Slow adaptive M-QAM with diversity in fast fading and shadowing," *IEEE Trans. Commun.*, vol. 55, no. 5, pp. 895 –905, May 2007.

[12] L. Jacobs and M. Moeneclaey, "Effect of MMSE channel estimation on BER performance of orthogonal space-time block codes in Rayleigh fading channels," *IEEE Trans. Commun.*, vol. 57, no. 5, pp. 1242–1245, May 2009.

[13] L. Toni and A. Conti, "Does fast adaptive modulation always outperform slow adaptive modulation?" *IEEE Trans. Wireless Commun.*, accepted for publication.

[14] A. Conti, M. Win, M. Chiani, and J. Winters, "Bit error outage for diversity reception in shadowing environment," *IEEE Commun. Lett.*, vol. 7, no. 1, pp. 15 – 17, Jan. 2003.

[15] A. Conti, M. Win, and M. Chiani, "On the inverse symbol-error probability for diversity reception," *IEEE Trans. Commun.*, vol. 51, no. 5, pp. 753–756, May 2003.

[16] C. Siriteanu and S. Blostein, "Performance and complexity analysis of eigencombining, statistical beamforming, and maximal-ratio combining," *IEEE Trans. Veh. Technol.*, vol. 58, no. 7, pp. 3383–3395, Sep. 2009.